Colloid Polym Sci 278:450–458 (2000)
© Springer-Verlag 2000

ORIGINAL CONTRIBUTION

S. Tang
C. M. McFarlane
Z. Zhang

Disruption of polystyrene latex aggregates in capillary flow

Received: 30 June 1999
Accepted in revised form: 11 November 1999

S. Tang (✉)
Department of Chemical Engineering and Chemical Technology
Imperial College, London SW7 2BY, UK
e-mail: s.tang@ic.ac.uk

C. M. McFarlane · Z. Zhang
School of Chemical Engineering
University of Birmingham
Birmingham B15 2TT, UK

Abstract Disruption of polystyrene latex aggregates, formed in 1 M citric acid/phosphate buffer solution at pH 3.8 through diffusion-limited colloid aggregation (DLCA) and in 0.2 M NaCl solution at pH 5.5 through reaction-limited colloid aggregation (RLCA), was studied with respect to aggregate size and fractal nature. This was achieved using small-angle laser scattering in conjunction with a specially designed sampling method, which brought about the elimination of the disruption of the aggregates caused by a commercial stirrer sample unit. Aggregations were carried out in a mixture of deuterium oxide and water instead of water alone as a solvent to minimise sedimentation resulting from the differences in density between the latex particles and the electrolytes. An initial "steady state" in terms of aggregate size and fractal dimension was found to occur after around 20 min and 2 days for DLCA and RLCA aggregates, respectively, at 25 °C. No aggregate disruption was detected for DLCA and RLCA aggregates after their passing through a capillary tube for shear rates up to 1584 and 2694 s^{-1}, respectively. At higher shear rates, significant decreases in the aggregate volume-mean diameter, $D[4, 3]$, occurred after shearing. The degree of reduction in $D[4, 3]$ was larger for DLCA aggregates in comparison to RLCA aggregates. The results would suggest that DLCA aggregates were more subject to disruption during shearing. A high degree of disruption was observed in turbulent flow for both aggregates.

Key words Disruption · Aggregates · Size · Fractal dimension · Capillary flow

Introduction

Aggregation is widely used in many industrial processes, such as water treatment, mineral recovery, paper manufacturing, enhanced oil recovery, and in bioprocesses as a means of enhancing solid/liquid separation rates. In most industrial applications, an increase in floc size and/or density is required to improve the efficiency of separation; however, in practice, an increase in aggregate size is generally accompanied by a reduction in aggregate density [1]. Aggregates are commonly considered to be fragile and can be disrupted during processing, for example, pumping and centrifugation. In order to minimise the disruption, it is essential to understand the mechanisms by which this takes place.

Colloidal aggregates formed by Brownian motion have previously been shown to be fractals [2]. Their structures can be characterised in terms of the fractal dimension, which describes how aggregate geometric properties change with their characteristic length. Two well-defined regimes of irreversible colloid aggregation have been identified: diffusion-limited colloid aggregation (DLCA) and reaction-limited colloid aggregation

(RLCA) [3]. DLCA occurs when there are negligible repulsive forces between the colloid particles; as a result, the particles are able to come together even closer than the thickness of the double layer under attraction forces, causing the particles to stick upon contact and form highly tenuous structures. In contrast, in RLCA a substantial repulsive force remains between the particles, so the particles may collide many times before sticking and the sticking probability approaches zero. The regimes are determined by the collision mechanism; experimentally the sticking probability can be varied by the addition of electrolytes into suspensions to eliminate or reduce the repulsive force between the particles [4].

The mechanisms involved in aggregate formation and breakup in laminar and turbulent flows are complicated since shear and differential sedimentation can also lead to particle collisions, resulting in formation and/or breakup of aggregates. Practically only one of these mechanisms is assumed to dominate, depending on particle size, temperature and shear rate [5]. Brownian motion is generally acknowledged to be important only for small particles (1 μm or smaller); both shear and differential sedimentation have been suggested as predominating in the flocculation of larger particles. As fluid shear changes the trajectories of the colliding particles and applies forces on the aggregates, the clusters are subject to fragmentation, eventually leading to a breakup of the aggregates [6].

Whether or not aggregates can survive during shearing depends on the resistance of the aggregates to hydrodynamic shearing forces, i.e., the mechanical strength of the aggregates. Aggregates have different strengths depending upon how well their component particles fit together. As particles grow by collision of particles because of Brownian motion their surface geometry becomes more complex resulting in a progressively poorer fit upon junction (contact) and progressively lower aggregate density [7]. In general, larger aggregates are weaker because of the poor fitting inherent with their formation [7, 8]. Theoretical models have also predicted that the aggregate tensile strength is inversely proportional to aggregate size [8, 9], although the aggregates were treated as porous but homogeneous structures neglecting a density gradient present.

Latex particles are widely used for investigating various aspects of colloidal and aggregation behaviour because of their initial monodispersity, chemical resistance and ability to be destabilised by salts. Latex particles are composed of a large number of polymer chains, with the individual chains having molecular weights in the range 10^5–10^7. Previous studies on latex aggregation have been done either in the aspect of size distributions [10–12] or fractal natures [6, 13–15]. However, a major problem could arise from the breakage of fragile aggregates either by the method of sampling or by measurement [16]. In this work, a new method was devised to introduce samples into the measurement cell of a Malvern Mastersizer [17] so as to eliminate the disruption of aggregates during size and fractal dimension measurements.

Whilst the shear-induced formation and breakup of latex aggregates has been studied in recent years [6, 14] and an investigation into the breakage of latex aggregates in laminar flow has been carried out previously by the authors [18], no result on the disruption of latex aggregates in turbulent capillary flow has been reported yet. The aim of this work was to systematically study the disruption of polystyrene latex aggregates in laminar and turbulent capillary flows in terms of aggregate size and fractal dimension. A small-angle laser light scattering method was used for measuring the aggregate size and fractal dimensions of latex aggregates.

Materials and methods

Polystyrene latex particles

The surfactant-free zwitterionic polystyrene latex particles used in this work (batch no. 719) were purchased from the Interfacial Dynamics Corporation, Portland, Ore., USA. The number-mean ($D[1, 0]$) and volume-mean ($D[4, 3]$) diameters of the single particles were 1.11 and 1.18 μm $\pm$ 0.01 (standard error) measured using a Malvern Mastersizer S (Malvern Instruments, UK). The isoelectric point of the latex particles was estimated to be about pH 3.1 by measuring the electrophoretic mobilities of a series of latex dispersions at different ionic strengths and pH using a Zeta Master (ZEM 5000, Malvern).

Aggregate generation

The latex stock sample was placed in an T-9 ultrasonic bath (L&R Manufacturing Company, Jersey, USA) for about 20 min prior to aggregation, in order to break doublets in the suspensions [19]. Aggregates were generated using the zwitterionic latex particles as follows: 0.002% w/v latex in 1.0 M citric acid/phosphate buffer at pH 3.8 (DLCA); 0.008% w/v latex in 0.2 M NaCl solution at pH 5.5 (RLCA). The buffer solutions were composed of sodium hydrogen orthophosphate citric acid and potassium chloride [20]. The aggregate suspensions were mixed by swirling gently 10 times at 33 rpm using an SB1 blood tube rotator (Stuart Scientific, UK) and were placed in a water bath at 25 °C. In order to minimise particle sedimentation, aggregation was carried out in a mixture of deuterium oxide (54%)/water (46%)/electrolyte having a density of 1.055 g cm^{-3} identical to that of the latex particles.

A capillary device

A capillary flow apparatus (Fig. 1) which consisted of a reservoir and a capillary test section connected by wide-bore silicone tubing [21] was used to study aggregate disruption as a function of shear rate. The capillary tube had an internal diameter of 1.1 mm and a length of 22 mm and was in turn connected via wide-bore silicone tubing to the measurement cell of the Malvern Mastersizer. Flow rates through the capillary tube were adjusted via a variable speed pump on the outlet of the Malvern Mastersizer.

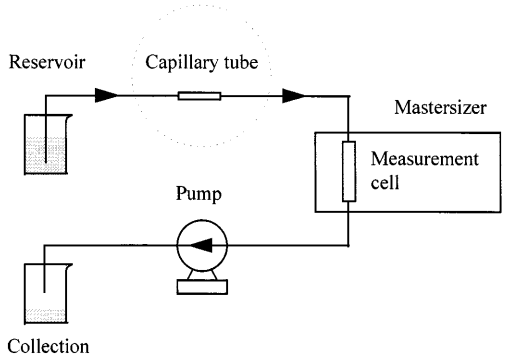

Fig. 1 Schematic of the disruption apparatus

Aggregate size measurement

A Malvern Mastersizer in conjunction with a specially designed sampling method (outlet pumping) was used in this work [17]. A pump (Watson-Marlow 501 U) was connected to the Mastersizer with wide-bore silicone tubing (4.8-mm internal diameter). During measurements, suspensions were sucked into the Malvern optical cell at a very low flow rate of 4.60×10^{-7} m^3 s^{-1} (shear rate about 4 s^{-1}) by using the pump. This newly designed sampling method was found to cause no damage to the latex aggregates being measured.

Fractal dimension

The fractal dimension (D_3) of the latex aggregates was obtained from the slope of the logarithmic plot of scattering intensity (I) against wave vector (Q), because the scattering intensity of the waves scattered from an aggregate obeys a power law in the magnitude of the wave vector (at a given scattering angle one probes fluctuations of Fourier spatial frequency) [22]

$$I \propto Q^{-D_3} \quad , \tag{1}$$

where Q is a function of the scattering angle (θ) and the wavelength (λ) of laser light; i.e., $Q = (4\pi n/\lambda)\sin(\theta/2)$, where n is the refractive index of the medium. The angular dependency of the scattering intensity of the latex aggregate samples was measured using a Malvern Mastersizer S [17] consisting of a 5-mW He–Ne laser with a wavelength of 632.8 nm, an optic lens (300RF) and 45 photosensitive detectors which allow the collection of light scattered at angles from 0.03° to 46.4°.

Image analysis

The image analysis system (Quantimet 500, Germany), consisting of a microscope (Leica DMR, Germany) and a charge-coupled-device (CCD) video camera (Sony, Japan), was used to take images of the latex aggregates. Images from the CCD video camera focused through the microscope were fed to a personal computer for image analysis [23].

Results and discussion

Growth of latex aggregates

As the repulsive forces between particles are negligible for DLCA, the rate of aggregation is solely limited by the time taken for clusters, and/or particles to encounter each other by diffusion. $D[1, 0]$ and D_3 of 0.002% w/v DLCA latex aggregates formed in 1 M citric acid/phosphate buffer are shown in Fig. 2. Six samples of latex aggregates were measured at each time and the error bars indicated in the figure represent the standard errors between the samples. $D[1, 0]$ and $D[4, 3]$ were essentially constant during the time of the experiment at 25 °C, with $D[1, 0] \sim 1.7$ μm. D_3 was found to be about 1.7, close to the D_3 value of 1.8 indicated for DLCA aggregates [13]. Hence it was considered that a "steady state" in terms of $D[1, 0]$ and D_3 existed after around 20 min until 6 h.

For RLCA, the aggregation rate was limited by the time taken for particles and/or clusters to overcome the low repulsive barrier by thermal activation before aggregation could proceed. A slightly higher solids concentration of latex of 0.008% w/v was employed to provide a higher collision frequency for the particles, ensuring the formation of aggregates in a reasonable time. As shown in Fig. 3, $D[1, 0]$ increased with time before reaching a plateau between 1.5 and 4 days with $D[1, 0] \sim 2$ μm; D_3 decreased starting from 2.9 (corresponding to single particles) during the first day and thereafter reached a plateau over 3 days with $D_3 \sim 2$, close to the value of 2.1 expected for RLCA aggregates [13]. The reduction in D_3 indicates that the population of single particles decreased with time whereas the formation of aggregates progressed. The period of 2–4 days is then considered as an initial "steady state" for the RLCA aggregates. The slight decrease in D_3 implies the formation of larger aggregates with loose structures. This may be a consequence of the formation of "colloidal gels" observed in the top part of the aggregate suspensions after 5 days.

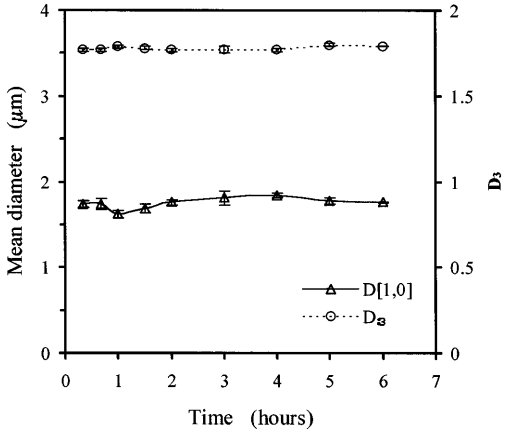

Fig. 2 Number-mean diameters, $D[1, 0]$, and fractal dimensions, D_3, of diffusion-limited colloid aggregation (*DLCA*) latex aggregates, formed in 1 M citric acid/phosphate buffer at pH 3.8, as a function of aggregation time

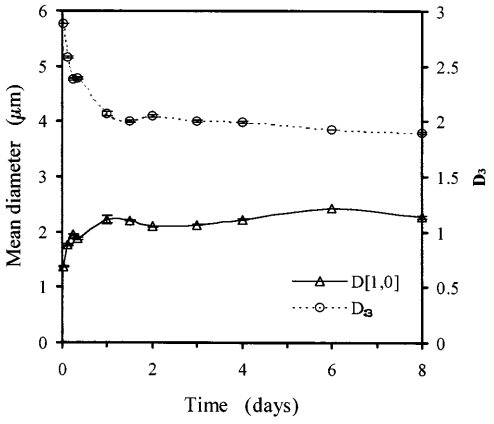

Fig. 3 $D[1, 0]$ and D_3 of reaction-limited colloid aggregation (*RLCA*) latex aggregates, formed in 0.2 M NaCl solution at pH 5.5, as a function of aggregation time

Characterisation of capillary flow

A number of experiments were made to assess whether differences in size and/or structure, arising from different aggregate formation mechanisms and collision efficiencies of particles, resulted in different degrees of disruption in laminar shear and turbulent shear.

A capillary tube with an interior diameter (D) of 1.1 mm and a length (L) of 22 mm was used in this work to provide laminar shear and turbulent shear. The flow rate (q) at which the aggregate suspensions passed through the capillary tube was adjusted to produce laminar and turbulent flows in the capillary tube with a series of Reynolds numbers ($Re = \rho u \mathrm{d}/\mu$, where u is the mean flow velocity, equal to $4q/\pi D^2$). The shear rate (γ) in the capillary tube can be predicted from Eq. (2) [21]

$$\gamma = (D/4\mu L)\Delta P \ , \tag{2}$$

where μ is the viscosity of the fluid, L the length of the capillary and ΔP the pressure drop in the capillary tube. The pressure drop in capillary laminar flow may be calculated from the Hagen–Poiseuille equation [24]:

$$\Delta P = 128\,\mu L q/\pi D^4 \ . \tag{3}$$

For capillary turbulent flow, assuming flat-plate theory, ΔP is given by [21]

$$\Delta P = 2.413 \rho Re^{-0.2} L^{0.8} D^{-4.8} q^2 \ , \tag{4}$$

where ρ is the density of the fluid. The estimated values of the shear rates for the capillary tube at different flow rates are summarised in Table 1. The flow with $Re > 2000$ is considered as turbulent for the capillary tube [25]. The energy dissipation rate in the turbulent region (ε) is estimated by

Table 1 Characterisation of a capillary tube

Flow rate ($m^3\ s^{-1}$)	Reynolds number	Shear rate (s^{-1})	Type of flow
6.18×10^{-8}	72	473	Laminar
2.07×10^{-7}	240	1584	Laminar
3.52×10^{-7}	407	2694	Laminar
7.37×10^{-7}	853	5640	Laminar
1.33×10^{-6}	1539	10178	Laminar
1.94×10^{-6}	2245	26928	Turbulent
2.59×10^{-6}	2998	45300	Turbulent
4.10×10^{-6}	4745	104000	Turbulent

$$\varepsilon = \frac{(4/\pi)q\Delta P - \mu L\gamma^2\left[D^2 - \left[D - 5v(D/\mu L\Delta P)^{0.5}\right]^2\right]}{\rho D^2 L} \ , \tag{5}$$

where v is the kinematic viscosity of the medium, equal to $0.99 \times 10^{-6}\ m^2\ s^{-1}$ (assuming waterlike properties of the media). Hence, the Kolmogorov microscale of turbulence (λ') can be given by

$$\lambda' = (v^3/\varepsilon)^{1/4} \ . \tag{6}$$

Disruption of DLCA latex aggregates

Disruption experiments on DLCA latex aggregates were conducted 20 min after aggregate generation since after this time measurements of $D[1, 0]$ and D_3 showed steady values. Following initial measurement of these parameters, aggregate suspensions were passed through the turbulent capillary tube and then introduced directly into the sample unit of the Malvern Mastersizer for further measurements on their size and fractal dimension (Fig. 1). At least three samples of aggregate suspensions were passed through the capillary tube at each shear rate, so as to minimise the measurement errors resulting from both the generation and measurement of the aggregates.

$D[4, 3]$ and $D[1, 0]$ for 24 samples of DLCA aggregates at 20 min before shear were determined to be 15.83 ± 0.56 and 1.49 ± 0.02 μm respectively, showing a high degree of reproducibility in both the generation and measurement of the aggregates. The percentage changes in aggregate $D[4, 3]$ and $D[1, 0]$ of the DLCA latex aggregates aged 20 min before and after shearing are shown in Fig. 4. At the lowest shear rate of 473 s^{-1}, no obvious changes in either $D[4, 3]$ or $D[1, 0]$ were detected; the slight increases in $D[4, 3]$ and $D[1, 0]$ after shearing (less than 3%) can be attributed to the measurement errors, which were estimated to be about 5% and 3% for $D[4, 3]$ and $D[1, 0]$, respectively. $D[4, 3]$ of the aggregates decreased dramatically after shearing

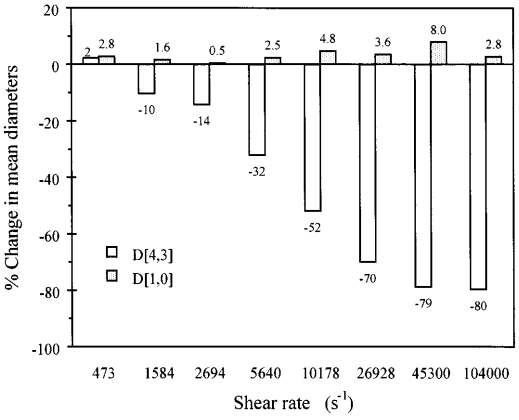

Fig. 4 Effect of laminar and turbulent shear on the volume-mean diameter, $D[4, 3]$, and $D[1, 0]$ of DLCA latex aggregates aged 20 min, formed in 1 M citric acid/phosphate buffer at pH 3.8

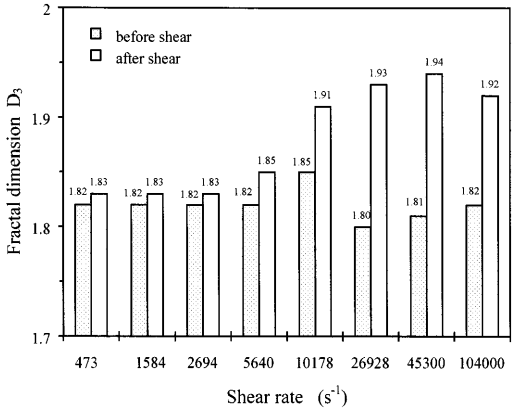

Fig. 5 Effect of laminar and turbulent shear on D_3 of DLCA latex aggregates aged 20 min, formed in 1 M citric acid/phosphate buffer at pH 3.8

at shear rates greater than or equal to 1584 s^{-1}, implying the disruption of larger aggregates during shearing. The reduction in $D[4, 3]$ increased with increasing shear rate, reaching a level higher than 70% for shear rates greater than or equal to 26928 s^{-1}. This is consistent with the expectation that aggregates should be more vulnerable to disruption at higher shear rates.

In contrast to $D[4, 3]$, $D[1, 0]$ remained relatively constant for shear rates less than 10178 s^{-1} after shearing (Fig. 4), when taking the measurement errors into account, suggesting that those aggregates which were broken during passage through the capillary are likely to have been the largest aggregates and represented a small proportion of the total aggregate population. The slight increase in $D[1, 0]$ for shear rates above 10178 s^{-1} was a consequence of large aggregates being broken into small aggregates with diameter slightly larger than the original $D[4, 3]$.

Whilst measuring aggregate size, the scattering intensity data required for determining fractal dimension were collected simultaneously. D_3 of the DLCA aggregates before and after their passing through the capillary tube is shown in Fig. 5. Standard errors of about 0.01 were estimated for measurements of D_3. No significant change in D_3 was observed for shear rates less than 5640 s^{-1}; thereafter D_3 increased to 1.94. The increase in D_3 would imply the formation of slightly compact, smaller aggregates and/or the reappearance of single particles resulting from the breakage of larger aggregates during shearing. Since $D[1, 0]$ of the aggregates (Fig. 4) either did not change significantly after shearing or showed a slight increase, the formation of more compact aggregates was the most likely reason for the increases in D_3.

Based on changes both in aggregate size and in fractal dimension, it is shown that a high degree of disruption of the DLCA aggregates occurred in turbulent flows with high shear rates. Aggregate disruption most likely took place in a very small region close to the capillary wall where local energy dissipation rates could be higher [22, 25]. The results are also consistent with the prediction that aggregates can be disrupted when the Kolmogorov microscale of turbulence (ranging from 5.54 to 9.43 μm for latex aggregates here, calculated using Eq. (6)) is compatible with the aggregate size [1, 21, 26].

The DLCA aggregates aged 6 h presented great similarities in the changes of diameters and fractal dimension. This showed a high reproducibility in the disruption experiments.

Disruption of RLCA latex aggregates

Similar disruption experiments were carried out for RLCA latex aggregates formed in 0.2 M NaCl solution at pH 5.5. Aggregate suspensions were passed through the capillary tube at a series of flow rates.

$D[4, 3]$ and $D[1, 0]$ for 24 samples of RLCA latex aggregates aged 2 days before passage through the capillary tube were measured to be 4.42 $\pm$ 0.05 and 2.07 $\pm$ 0.03 μm, respectively; the relative errors in determining $D[4, 3]$ and $D[1, 0]$ were estimated to be about 2.5% and 3%. The results indicate a high degree of reproducibility in both the generation and measurement of the aggregates.

The changes in $D[4, 3]$ and $D[1, 0]$ of the RLCA aggregates aged 2 days before and after shearing are shown in Fig. 6. No significant changes in either $D[4, 3]$ or $D[1, 0]$ were detected at shear rates of 473 and 1584 s^{-1}; however, for shear rates of 2694 s^{-1} or higher $D[4, 3]$ decreased progressively, implying breakup of aggregates. The reduction in $D[4, 3]$ reached about 66% at the highest shear rate of 104000 s^{-1}, showing a high degree of disruption of the aggregates occurred in turbulent flows.

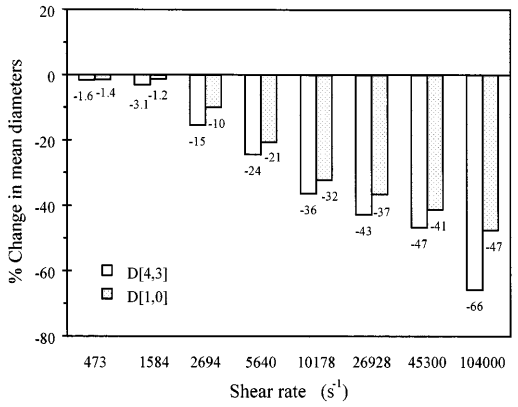

Fig. 6 Effect of laminar and turbulent shear on $D[4, 3]$ and $D[1, 0]$ of RLCA latex aggregates aged 2 days, formed in 0.2 M NaCl solution at pH 5.5

In contrast to DLCA aggregates, for which $D[1, 0]$ remained constant or showed a slight increase after shearing, $D[1, 0]$ of RLCA aggregates decreased substantially after shearing for shear rates greater than or equal to 2694 s^{-1}, as shown in Fig. 6. This would suggest that the larger aggregates were being disrupted into smaller aggregates with diameters smaller than the original $D[1, 0]$. The percentage reduction in $D[1, 0]$ increased with increasing shear rate; at the highest shear rate of 104000 s^{-1}, $D[1, 0]$ was reduced to about 1.26 μm, close to $D[1, 0]$ of single latex particles (about 1.11 μm). This implies the presence of a large population of single particles resulting from breakage of large aggregates.

The changes in D_3 of the RLCA aggregates aged 2 days before and after shearing are shown in Fig. 7. The standard error was estimated to be about 0.03. No noticeable changes were observed in D_3 at low shear rates less than 2694 s^{-1}, when taking the measurement errors into account. For shear rates of 2694 s^{-1} or higher the fractal dimensions increased significantly after shearing. The increase in D_3 was indicative of the increase in the proportion of single particles and/or the formation of more compact, smaller aggregates resulting from breakage of larger aggregates during shearing. A large increase in D_3 to 2.44 was found after shearing at 104000 s^{-1}, as a consequence of the formation of a large population of single latex particles. This can be seen in the number-based size distributions of latex aggregates before and after shearing at different shear rates in the capillary, as shown in Fig. 8. For a shear rate of 104000 s^{-1} there was a large shift in the size distribution such that there was significant overlap with the size distribution for a suspension of single latex particles, which had the same solid concentration of latex (0.008%), indicating a large proportion of single latex particles in the sheared aggregate suspensions. Therefore, the large increase in D_3 in turbulent flows was mostly due to the reappearance of single particles resulting from breakage of large aggregates during shearing. This was also confirmed by the fact that $D[4, 3]$ after shearing at 104000 s^{-1} was reduced to about 1.21 μm, close to that of latex single particles (1.18 μm).

Disruption experiments were also conducted for RLCA latex aggregates aged 1 day and 6 days so as to discover how time (ageing) influences the disruption of aggregates. All the aggregates presented very similar trends in the changes of mean diameters and fractal dimension with varying shear rate. No significant differences in the reductions in $D[4, 3]$ and $D[1, 0]$ were found for the aggregates aged for different days when taking the standard errors into account. Comparisons of the changes in D_3 of RLCA latex aggregates aged 1, 2 and 6 days before and after shearing are shown in Fig. 9 D_3 increased after shearing, which was indicative of the formation of more compact aggregates and single

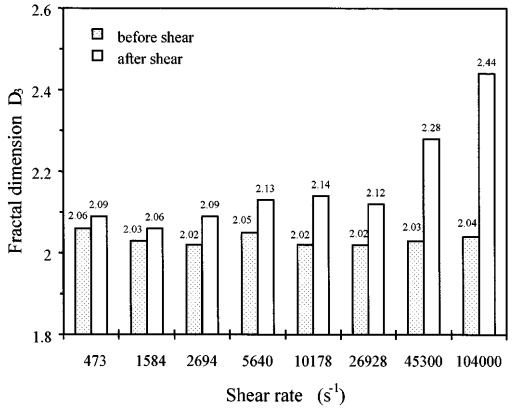

Fig. 7 Effect of laminar and turbulent shear on D_3 of RLCA latex aggregates aged 2 days, formed in 0.2 M NaCl solution at pH 5.5

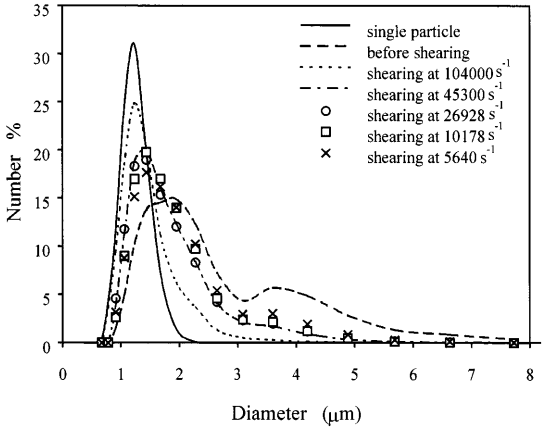

Fig. 8 Number-based size distributions of single latex particles and RLCA latex aggregates aged 2 days before and after shearing at a series of shear rates in capillary flow

particles; and the increases in D_3 increased with shearing rate. The degree of increase in D_3 after shearing is in the order 6 days > 2 days > 1 day, especially at higher shear rates. This can be explained in terms of the population of single latex particles, i.e., for the aggregates aged 6 days the largest number of single particles are "released" from the aggregates after shearing, as all of the aggregates aged different days presented similarities in the percentage changes of aggregate diameters before and after shearing.

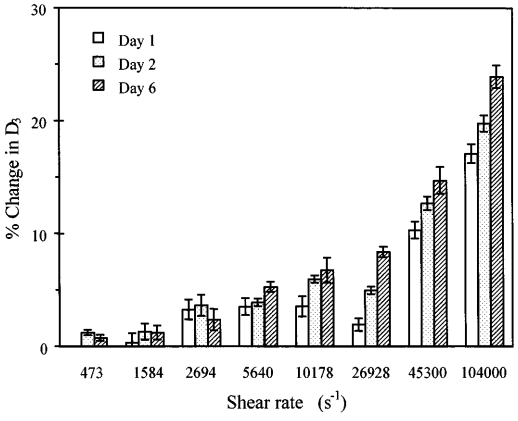

Fig. 9 Effect of shear on D_3 of DLCA latex aggregates aged 1, 2 and 6 days, formed in 0.2 M NaCl solution at pH 5.5

Prediction of aggregate strengths

The structures of DLCA and RLCA latex aggregates were observed using image analysis. The images clearly showed aggregate growth during the time course for RLCA aggregates (Fig. 10). It was found that the majority of the DLCA aggregates possessed a tenuous structure, while the RLCA ones were more compact. This is consistent with theoretical expectation and

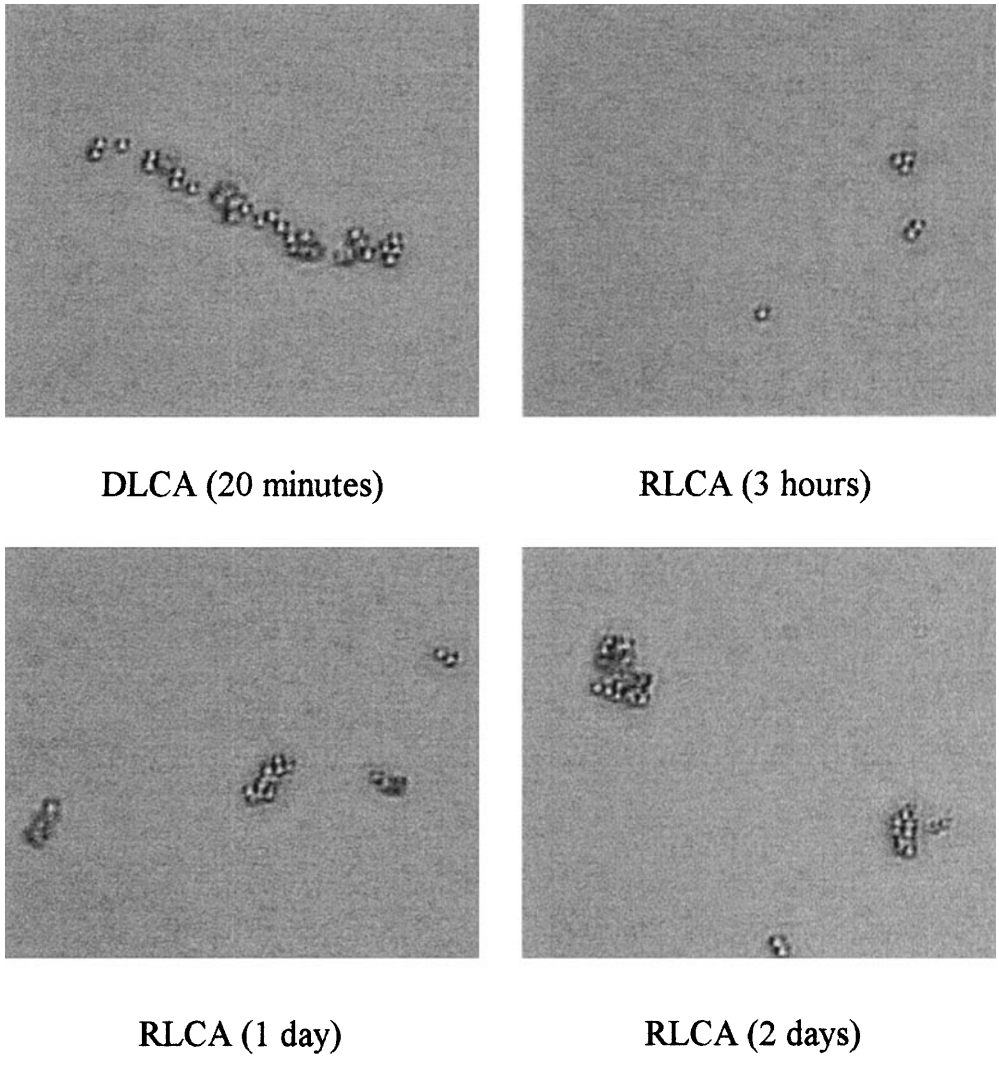

Fig. 10 Images of RLCA and DLCA latex aggregates taken using image analysis (magnification ×400)

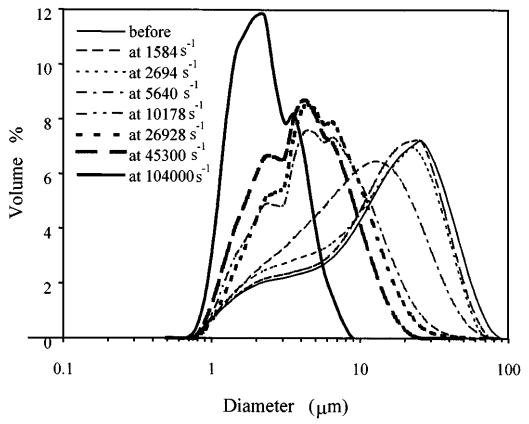

Fig. 11 Volume-based size distributions of DLCA latex aggregates aged 2 days before and after shearing at a series of shear rates in capillary flow

indicative of their fractal nature [2, 22]. From size distribution measurements DLCA > RLCA. Based on these findings it is anticipated that the larger, less compact DLCA aggregates are more susceptible to breakage during shearing.

The results described in the previous sections showed that for DLCA latex aggregates aged for 20 min $D[4, 3]$ began to decrease at a shear rate of 1584 s^{-1}, whereas no breakage was detected for RLCA latex aggregates until the shear rate reached 2694 s^{-1}. This is further indicated by changes in the size distributions of the aggregates. As shown in Fig. 11, the volume-based size distributions of DLCA latex aggregates shifted gradually to the left (low diameter) with increasing shear rate for shear rates of 1584 s^{-1}or higher, implying a gradual increase in the degree of disruption of larger aggregates. For RLCA aggregates, the volume-based size distribution had the identical shape until shear rates equal to 2694 s^{-1}; thereafter shifts in the size distribution to the left were observed. The results would suggest DLCA aggregates are more subject to disruption by shearing.

The degree of the reduction in $D[4, 3]$ of DLCA aggregates after shearing is larger in comparison to that of RLCA aggregates; the former reached about 80% while the latter less than 70%. One can expect that RLCA aggregates are more resistant to the extent of shearing.

In order to understand the disruption mechanisms further, the disruption results in terms of aggregate size and fractal dimension are to be linked to the mechanical strengths of both DLCA and RLCA latex aggregates, which are to be measured using micromanipulation with the aid of the novel design of Zhang et al. [27].

Conclusions

A Malvern Mastersizer in conjunction with a specially designed sampling method has been used for aggregate size and fractal dimension measurements. For DLCA, a "steady state" in terms of $D[1, 0]$ and D_3 existed after around 20 min until 6 h, with $D[1, 0] \sim 1.7$ μm and $D_3 \sim 1.8$. For RLCA, an initial "steady state" in terms of $D[1, 0]$ and D_3 was found to be in the range 2–4 days, with $D[1, 0] \sim 2$ μm and $D_3 \sim 2$.

Both DLCA and RLCA latex aggregates were found to be disrupted after passing through a capillary tube at higher shear rates. The changes in aggregate size showed a low degree of breakage of RLCA aggregates after shearing. This would suggest that RLCA aggregates had more or less high strength. Both DLCA and RLCA aggregates aged for different times presented great similarities in the changes of mean diameters and fractal dimension before and after shearing. Disruption results are to be related to the strength measurement using micromanipulation.

Acknowledgements The authors would like to thank J. M. Preece, H. Mashmoushy and M. Sisk for their help and/or useful discussion. Funding was provided by BBSRC.

References

1. Ayazi Shamlou P, Titchener-Hooker N (1993) In: Ayazi Shamlou P (ed) Processing of solid–liquid suspension. Butterworth-Heinemann, London, p 1
2. Pfeifer P, Obert M (1989) In: Avnir D (ed) The fractal approach to heterogeneous chemistry: surfaces, colloids, polymers. Wiley, New York, p 11
3. Weitz DA, Huang JS, Lin MY, Sung J (1985) J Phys Rev Lett 54:1416
4. Osipow LI (1962) Surface chemistry. Reinhold, New York, p 83
5. Hunt JR (1982) J Fluid Mech 122:303
6. Oles V (1992) J Colloid Surface Sci 154:351
7. Boadway JD (1978) J Environ Eng Div ASCE EE5:901
8. Muhle K (1993) In: Dobias B (ed) Coagulation and flocculation: theory and applications. M. Dekker, New York, p 355
9. Tambo N, Hozumi H (1979) Water Res 13:421
10. Pefferkorn E, Stoll S (1990) J Colloid Interface Sci 138:261
11. Stoll S, Pefferkorn E (1992) J Colloid Interface Sci 152:247
12. Stoll S, Pefferkorn E (1992) J Colloid Interface Sci 152:257
13. Lin MY, Lindsay HM, Weitz DA, Ball RC, Klein R, Meakin P (1989) Nature 339:360
14. Torres FE, Russel WB, Schowalter WR (1991) J Colloid Interface Sci 142:554
15. Tang S, McFarlane CM, Paul GC, Thomas CR (1999) Colloid Polym Sci 277: 325
16. Farrow J, Warren L (1993) In: Dobias O (ed) Coagulation and flocculation: theory and applications. Dekker, New York, p 391
17. Mashmoushy H, Tang S, Zhang Z, McFarlane CM, Thomas CR (1999) In:

Proceedings, Fifth International Conference on Fluid-Particle Interactions, May 9-14, Santa Fe, New Mexico
18. Tang S, Preece JM, McFarlane CM, Zhang Z (1999) J Colloid Interface Sci 221:114
19. Delgado A, Matijevic E (1991) Part Part Syst Charact 8:128
20. Elving PJ, Markowitz JM, Rosenthal I (1956) Anal Chem 28:1179
21. Zhang Z, Al-Rubeai M, Thomas CR (1993) Biotech Bioeng 42:987
22. Harrison A (1995) Fractals in chemistry. Oxford University Press, Oxford
23. Paul GC, Thomas CR (1998) In: Schuegerl K (ed) Relation between morphology and process performance. Advances in biochemical engineering/biotechnology, vol 60. Springer, Berlin Heidelberg, NewYork, p 1
24. Douglas JF, Gasiorek JM, Swaffield JA (1985) Fluid Mechanics. Pitman London, p 241
25. Davies JT (1972) Turbulent phenomena. Academic, New York
26. Thomas CR, Al-Rubeai M, Zhang Z (1994) Cytotechnol 15:329
27. Zhang Z, Ferenczi MA, Lush AC, Thomas CR (1991) Appl Microbiol Biotechnol 36:208